(2)

Naval Research Laboratory

Washington, DC 20375-5000

DTIC FILE COPY

NRL Memorandum Report 6273

AD-A200 382

The Design of a 100 GHz CARM Oscillator Experiment

R. B. McCOWAN

SAIC
McLean, VA

A. W. FLIFLET, S. H. GOLD AND A. K. KINKEAD

High Power Electromagnetic Radiation Branch
Plasma Physics Division

W. M. BLACK

High Power Electromagnetic Radiation Branch
Plasma Physics Division
and
Department of Electrical and Computer Engineering
George Mason University
Fairfax, VA

V. L. GRANATSTEIN

Department of Electrical Engineering
University of Maryland
College Park, MD

M. SUCY

JAYCOR, Inc.
Vienna, VA

September 14, 1988

Approved for public release; distribution unlimited.

88

SECURITY CLASSIFICATION OF THIS PAGE

REPORT DOCUMENTATION PAGE

Form Approved OMB No 0704-0188

1a REPORT SECURITY CLASSIFICATION UNCLASSIFIED	1b RESTRICTIVE MARKINGS
2a SECURITY CLASSIFICATION AUTHORITY	3 DISTRIBUTION/AVAILABILITY OF REPORT Approved for public release; distribution unlimited.
2b DECLASSIFICATION/DOWNGRADING SCHEDULE	
4 PERFORMING ORGANIZATION REPORT NUMBER(S) NRL Memorandum Report 6273	5 MONITORING ORGANIZATION REPORT NUMBER(S)
6a NAME OF PERFORMING ORGANIZATION Naval Research Laboratory — 6b OFFICE SYMBOL (If applicable) Code 4740	7a NAME OF MONITORING ORGANIZATION
6c ADDRESS (City, State, and ZIP Code) Washington, DC 20375-5000	7b ADDRESS (City, State, and ZIP Code)
8a NAME OF FUNDING/SPONSORING ORGANIZATION — 8b OFFICE SYMBOL (If applicable)	9 PROCUREMENT INSTRUMENT IDENTIFICATION NUMBER
8c ADDRESS (City, State, and ZIP Code)	10 SOURCE OF FUNDING NUMBERS PROGRAM ELEMENT NO — PROJECT NO — TASK NO — WORK UNIT ACCESSION NO

11 TITLE (Include Security Classification)
The Design of the 100 GHz CARM Oscillator Experiment

12 PERSONAL AUTHOR(S)
(See page ii)

13a TYPE OF REPORT	13b TIME COVERED	14 DATE OF REPORT (Year, Month, Day)	15 PAGE COUNT
	FROM ____ TO ____	1988 September 14	31

16 SUPPLEMENTARY NOTATION
(See page ii)

17 COSATI CODES			18 SUBJECT TERMS (Continue on reverse if necessary and identify by block number)
FIELD	GROUP	SUB-GROUP	

19 ABSTRACT (Continue on reverse if necessary and identify by block number)

The design of a 10-20 MW, 40 nsec cyclotron auto-resonance maser is presented. The basic components of the CARM are a pulseline accelerator, magnetic-field coils, a novel 600 kV, 200 A field-emission electron gun designed for $p_\perp / p_z = 0.6$ and $\Delta p_z / p_z < 3\%$, and a "whispering-gallery" mode rippled-wall cavity designed for high Q for the desired CARM mode and for low Q for competing gyrotron interactions. The NRL CARM operates with a wave group velocity that is less than optimum for autoresonance, but where the cyclotron maser instability is strong. By keeping the interaction region short (less than 10 cyclotron orbits), the effect of velocity spread is reduced, and the efficiency can be quite high; computer simulations indicate that the device will operate at efficiencies greater than 20%

20 DISTRIBUTION/AVAILABILITY OF ABSTRACT ☒ UNCLASSIFIED/UNLIMITED ☐ SAME AS RPT ☐ DTIC USERS	21 ABSTRACT SECURITY CLASSIFICATION UNCLASSIFIED	
22a NAME OF RESPONSIBLE INDIVIDUAL Arne W. Fliflet	22b TELEPHONE (Include Area Code) (202) 767-2469	22c OFFICE SYMBOL Code 4740

DD Form 1473, JUN 86 — Previous editions are obsolete — SECURITY CLASSIFICATION OF THIS PAGE

S/N 0102-LF-014-6603

12. Personal Author(s)

Granatstein,* V.L., Sucy,** M., McCowan,+ R.B., Fliflet, A.W. Gold, S.H., Black,++ W.M., Manheimer, W.M. and Kinkead, A.K.

16. SUPPLEMENTARY NOTATION

*Department of Electrical Engineering, University of Maryland, College Park, MD
**JAYCOR, Inc., Vienna, VA
+SAIC, McLean, VA
++Department of Electrical and Computer Engineering George Mason University, Fairfax, VA

CONTENTS

THE DESIGN OF A 100 GHZ CARM OSCILLATOR EXPERIMENT

I. Introduction

High-power millimeter waves have many important applications. For example, millimeter-wave radar systems will yield higher target resolution than lower-frequency systems for a particular antenna aperture. Communications systems may benefit from a more strongly-focused radiation beam and from the larger information bandwidth available as the frequency is increased. Electron-cyclotron-resonance heating of fusion plasmas will require high-frequency radiation when strong magnetic fields are used to confine the plasma.[1]

The cyclotron auto-resonance maser (CARM) is a promising source of high-power radiation in the 100 GHz to 500 GHz frequency range that may impact the requirements of advanced systems for applications such as those mentioned above. The requirements for guide magnetic-field strength and electron energy in a CARM may be advantageous when compared with competing devices. Compared with a gyrotron, the required magnetic field strength requirement is substantially reduced. The CARM can provide mm and sub-mm radiation in the first electron-cyclotron harmonic using currently available magnet technology. For example, the experiment at the Naval Research Laboratory is designed to produce powers in excess of 10 MW at 100 GHz with a 600 kV beam and a magnetic field of only 25 kG, while a first-harmonic gyrotron operating at 100 GHz with the same beam voltage requires a magnetic field of over 70 kG. Compared with a conventional magnetostatic-wiggler FEL, the CARM can reach sub-mm wavelengths with a lower electron-beam voltage. For example, a 500 kV CARM oscillator has the potential for efficient multi-MW operation at wavelengths down to 0.75 mm with a 100 kG superconducting magnet; a 500 kV FEL oscillator with a 3 cm period magnetic-wiggler will produce radiation at 4.5 mm.[2]

The CARM can be either an amplifier or an oscillator. An oscillator design removes the need for an input source and input couplers. In addition, amplifier operation requires suppression of backward-wave instabilities.

The CARM oscillator, like the gyrotron oscillator, is a cyclotron maser. In contrast to the gyrotron, which requires an electron beam with a large momentum pitch angle (typically $p_\perp/p_z > 1$), the CARM has an electron beam with a low to moderate pitch angle ($p_\perp/p_z < 0.7$) and a substantial amount of axial momentum. The CARM benefits from the doppler upshift provided by the axial velocity of the beam: the operating frequency of the CARM is approximately $\gamma^2 f_c$, where f_c is the relativistic cyclotron frequency associated

Manuscript approved June 21, 1988.

with the axial magnetic field, and γ is the usual relativistic factor. The dispersion relation for the NRL CARM is shown in Fig. 1. The CARM interaction corresponds to the upper intersection of the beam cyclotron mode and the waveguide mode.

There is a fairly extensive literature on the theory and simulation of CARMs and other doppler-shifted cyclotron maser configurations [3]-[10]. The only experimental studies reported to date, however, have been the experiments of Botvinnik et al [11],[12], who achieved 6 MW at a wavelength of 4.3 mm and 4% efficiency, and 10 MW at a wavelength of 2.4 mm and 2% efficiency. A major objective of the present experiment is the achievement of higher efficiency, ~20%, which is predicted by theory for the CARM.

Fig. 2 shows the important components of the experiment. The electron beam is launched from the velvet emitter surface into a uniform magnetic field provided by the gun solenoid. A magnetic kicker supplies transverse momentum. Adiabatic compression in the input taper region increases the momentum pitch ratio to 0.6 in a magnetic field of 24 kG. The beam generates microwaves in a Bragg cavity[13], and is collected on the wall of the output taper.

Competition between the desired mode and other available modes can lead to unstable operation; the density of modes which can be excited by the CARM interaction is generally high. In addition, gyrotron modes, which are nearly cut-off and operate near the cyclotron frequency, also present significant competition. Electron beam velocity spread, which leads to lowered efficiency, is also a critical factor in the design of a CARM oscillator. This paper presents the design of an electron gun and a microwave resonator to achieve a highly efficient CARM.

II. Design of the Bragg cavity

In order that the CARM oscillate in the correct mode at the Doppler-shifted frequency, the oscillation-threshold current of the CARM mode should be lower than the threshold currents of competing modes. The cavity and beam parameters chosen for this experiment are based on the theoretical study of the CARM interaction given in Ref. 14. As shown in that paper, the efficiency of the CARM is optimized by choosing a normalized interaction length $\mu = 8$, and a normalized wave amplitude $F = 0.2$, where μ and F are defined below.

$$\mu \equiv \frac{\beta_{\perp o}^2}{2} \frac{1 - \beta_{ph}^{-2}}{1 - \beta_z/\beta_{ph}} \frac{\omega L}{c}, \tag{1}$$

and,

$$F \equiv \frac{4k_z}{\gamma_o m_o c^2} \frac{C_{mn} J_{m-s}(k_{mn} r_o) \times \left(1 - \beta_z/\beta_{ph}\right)}{2\beta_{\perp o}^3 \left(1 - \beta_{ph}^{-2}\right)} \Pi, \tag{2}$$

where Π is the mode-equivalent-voltage amplitude[12], β_z is the axial velocity of the electrons, β_{ph} is the phase velocity of the radiation, k_{mn} is the wave number of the radiation, r_o is the mean radius of the electron beam, $\beta_{\perp o}$ is the transverse velocity of the electrons, L is the length of the cavity, ω is the angular frequency of the radiation, and C_{mn} is a beam-wave coupling coefficient that depends on the mode indices.[15]

Gyrotron modes are the most dangerous competing modes because the gyrotron interaction is the strongest cyclotron-maser interaction; the cavity must be kept short to raise the threshold currents of the gyrotron modes. The Q of the resonator is 1500 for the design mode, which makes the oscillation threshold current for the CARM approximately 50 Amp; the gyrotron interaction must have a higher start current. In order to minimize the total cavity length, the reflectors must be short.

A cavity design that satisfies the criteria for a CARM oscillator is the Bragg cavity. The Bragg cavity is a section of smooth waveguide connecting two rippled-waveguide reflectors[13]. For the proper mode, for which the guide wavelength is twice the ripple period, constructive interference of the small reflections from the ripples can provide a strong reflection. Whispering-gallery (TE_{m1}) modes couple most strongly to the corrugations[16], and therefore have the highest reflectivities. Other modes can have low reflectivity. The Q of the resonator can be increased either by lengthening the uncorrugated section, or by increasing the reflectivity of the corrugated sections. Since each reflector provides a 90° phase shift, the length of the smooth section must be such that the total path length of the radiation in one round trip of the resonator is an odd integral number of half wavelengths.

If the corrugated sections are highly reflective, the Q of the Bragg resonator is

$$Q = \frac{k^2 L_{eff}}{k_z(1 - R_1 R_2)} \tag{3}$$

where k is the free-space wave number, k_z is the waveguide axial wave number, and R_1 and R_2 are the reflectivities of the corrugated sections which are given by

$$R = \mathrm{Tanh}^2\, GL. \tag{4}$$

L_{eff} is the effective length of the cavity, which is larger than the length of the smooth-waveguide section because of the energy stored in the rippled-waveguide sections.

$$L_{eff} = L_0 + \frac{1}{G_1}\left(1 - e^{-G_1 L_1}\right) + \frac{1}{G_2}\left(1 - e^{-G_2 L_2}\right), \tag{5}$$

where L_1 and L_2 are the lengths of the reflectors; G_1 and G_2, are the coupling coefficients of the reflectors and are

$$G = \frac{l_0}{2}\left\{\frac{x'^4_{mn} - m^2a^2\left(\omega^2/c^2 + \beta^2\right)}{\beta a^3\left(x'^2_{mn} - m^2\right)}\right\} \tag{6}$$

for the TE modes, and

$$G = \frac{l_0}{2a}\frac{\omega^2/c^2 + \beta^2}{\beta} \tag{7}$$

for the TM modes[3],[16]. l_0 is the length of the rippled section, x'_{mn} is the zero of the derivative of the Bessel function with respect to its argument, m as the azimuthal index, a is the waveguide wall radius, ω is the angular frequency, β is the wave number of the radiation, and c is the speed of light.

In order for the device to work successfully as a CARM, the threshold currents of gyrotron modes must be greater than the threshold current of the desired CARM mode. The CARM has a beam with a low to moderate ratio (α) of transverse momentum to axial momentum, which raises the threshold current of the gyrotron modes. Even so, the Q of the gyrotron modes must be kept as low as possible, which means the cavity must be kept as short as possible. The smallest possible Q of a gyrotron mode in a straight cavity of length L_0 is the minimum diffraction Q:

$$Q_{min} = \frac{4\pi}{p}\left(\frac{L_0}{\lambda_{fs}}\right)^2, \tag{8}$$

where λ_{fs} is the free-space wavelength of the near-cutoff mode, and p is the number of half wavelengths in the cavity. The shorter the cavity, the less dangerous the gyrotron modes.

Table I summarizes the design of the cavity for the NRL 100 GHz experiment, and Fig 3 shows the relationship between the cavity geometry and the radiation envelope. The Q of the resonator for the CARM must be high enough to ensure that that competing gyrotron modes will not start before the CARM mode starts. For the parameters of the NRL experiment,the highest Q gyrotron mode has a Q of approximately 500. In order to satisfy the requirement that the CARM mode oscillates at a lower current than any competing gyrotron mode, the Q of the CARM operating mode must exceed 1400. Since a reflectivity of 90% was chosen for the downstream reflector and a reflectivity of 98% was chosen for the upstream reflector, the smooth section of the resonator must be 2.5 cm long. The upstream reflector is the shallower of the two corrugated sections, and hence has the longer radiation e-folding length. The upstream and downstream reflectors are 3 cm and 1.5 cm long respectively.

The time dependence of the CARM oscillator driven by a pulsed-power system must be considered. A model of the voltage pulse that consists of a linear voltage rise from zero to the operating voltage, followed by a constant voltage for the rest of the pulse was chosen to be used in a single-mode, time-dependent, fixed-field CARM oscillator code.

The results of this code, shown in fig 4, indicate that a 70 nsec pulse is more than adequate to drive the CARM mode to saturation. In addition, the start-up of the various cavity modes during the rise of the pulse must be considered. Fig 5 shows a plot of the start current for the modes in the Bragg cavity for a beam with the parameters outlined in the next section. The starting currents are calculated for a fixed field profile and for voltages ranging from 0 to 700 kV, while the magnetic field is kept constant. α is assumed proportional to V. The current in the beginning of the pulse is assumed to vary as the voltage to the 3/2 power in order to model space-charge limited flow from a relativistic diode.. As the current rises in the pulse, the TE_{81} mode is expected to start first, followed by the TE_{71}, which is followed by the TE_{61} mode. The major competing gyrotron modes are also plotted; they are denoted by the dashed line.

The ohmic Q of the cavity is approximately 16000[16]. For a 10 MW output power, approximately 1 MW is dissipated by wall currents. Since the cavity wall has an effective area of 20 cm^2, the power density dissipated by wall currents is 50 kW/cm^2, acceptable only for short-pulse, low-duty-factor operation.

III. The CARM electron beam requirements

For the NRL 100 GHz, 10 MW CARM design, the requirements for the electron beam are unique. A 600 kV, 200 A. electron beam is needed for optimum efficiency with the present cavity design. The beam requires transverse velocity $v_\perp/c \cong 1/\gamma$ to achieve high efficiency with significant Doppler upshift. Thus, for the current design, $\alpha \equiv v_\perp/v_\parallel \cong 0.6$. The waveguide mode is the TE_{61} whispering gallery mode, and has a group velocity of 0.89c. Although this group velocity is less than optimum for autoresonance, it leads to a short interaction length (approximately 8 cyclotron orbits) and reduced sensitivity to beam spread.

The constraint on beam axial-velocity spread can be estimated by a simple coherence argument, which leads to the condition $\Delta v_z/v_z < \lambda/2L$. The constraint on energy spread for a beam with no pitch angle spread is

$$\Delta\gamma/\gamma < \frac{1 - \gamma_o^{-2}}{(1 + \alpha^2)\left(\Omega/\omega - \gamma_o^{-2}\right)} \tag{10}$$

Nonlinear efficiency calculations indicate that if the velocity spread is within these constraints, the efficiency of the interaction will be degraded only slightly. According to Fig. 6, which plots the beam quality constraints, the interaction will be unaffected if the axial velocity spread is kept less than 3%. These curves also show that there is greater sensitivity to pitch-angle spread than to energy spread, a feature related to the auto-resonant character of the interaction.

Fig. 7, which shows the coupling strength[15] of the TE_{61} mode as a function of radial beam position, demonstrates that the beam must have most of the current concentrated near the wall in order that it interact strongly with the operating mode.

The electron gun is designed to produce a high-quality electron beam without requiring beam scraping. The electrode shapes are chosen to compensate for space-charge repulsion within the electron beam. The beam is launched parallel to the guide magnetic field. Downstream from the diode, a nonadiabatic magnetic region provides the required transverse momentum. Separation of the beam formation stage from the transverse momentum pump allows each stage to be analyzed independently.

IV. Design procedure for the annular gun

The cold-cathode electron gun was designed in two steps: electrode synthesis, and validation of the synthesized electrodes with an electron trajectory code[17]. The approximate electrode shapes were determined using an electrode-synthesis technique[18]. The synthesis code calculates the charge distribution due to a space-charge-limited, laminar flow of electrons based on a one-dimensional, planar, relativistic model. From the charge distribution, the code determines the equipotentials by solving Laplace's equation in regions external to the beam. Electrodes are placed on these equipotentials. In order to predict the behavior of the electron beam in a realistic, two-dimensional cylindrical geometry, the electrode surfaces chosen for the gun were used in a number of electron trajectory code runs. The trajectory code is the best way to determine the velocity spread in the beam, as well as to determine the transverse momentum. Fig. 8 shows the shape of the cathode and anode.

The anode-cathode system designed by the above procedure produces a cold annular beam with negligible transverse momentum. In order to efficiently produce radiation, the present CARM oscillator requires an electron beam with $\alpha = 0.6$. Therefore it is necessary to impart transverse momentum to the beam. A magnetic kicker provides the required transverse momentum.

The magnetic kicker consists of a local depression of the axial magnetic field and is similar to the one used by Gold et. al[19] in the NRL high voltage gyrotron experiments. If the magnitude of the magnetic field changes on a length scale shorter than a cyclotron orbit, $(dB_z/dz)/B_z < 2\pi v_z/\omega_c$, beam axial momentum is converted to beam transverse momentum. A magnetic kicker is simple to construct: a coil is wound on a section of the vacuum vessel, and a current is driven through the coil to produce a field opposite in direction to the main axial field. The combination of the nearly cold beam followed by a magnetic kicker provides a flexible way to create an electron beam suitable for the CARM; proper choice of operating parameters will generate an electron beam with any α between 0.5 and 0.7, and an axial-velocity spread that shouldn't exceed 3%.

At the operating voltage of 600 kV, the electron emitter must provide uniform electron emission with an emitter surface field strength of 125 kV. At the same time, the focus electrodes, which are subjected to a field strength of 400 kV/cm, must withstand electrical breakdown. Therefore, the diode materials were carefully chosen. The emission surface is cotton velvet. The tufts of the velvet provide local enhancements to the electric field, and encourage electrical breakdown and plasma formation. Reliable emission at electric fields less than 100 kV/cm has been achieved using cotton velvet cathodes[20]. The velvet is attached to the aluminum cathode using silver-bearing epoxy.

The focus electrode is constructed of anodized aluminum. Hard coat anodization creates a corundum surface .002" thick. This surface will prevent emission at field strengths greater than 400 kV/cm, provided that the voltage pulse is less than 100 nsec long[21],[22]. Since the pulse length of the accelerator used for the CARM experiment is less than 70 nsec, the anodized surface will hold off all emission from the focus electrodes.

V. Summary

The basic design for the 100 GHz, 10 MW NRL CARM oscillator has been presented. The basic components of the CARM are a pulseline accelerator, a novel 600 kV, 200 A field emission electron gun designed for $p_\perp/p_z = 0.6$ and $\Delta p_z/p_z < 3\%$, and a "whispering gallery" mode rippled wall cavity. The oscillator is designed to operate at an efficiency of over 20%. Construction of the experimental apparatus is completed and the electron gun is undergoing preliminary tests.

VI. Acknowledgement

This work was supported by the Office of Naval Research

REFERENCES

1) Granatstein, V. L., 1988, *Proc. of the 1987 Particle Accelerator Conf.*, (Washington, D. C. IEEE)

2) Sprangle, P., Smith, R. A., and Granatstein, V. L., 1979, in *Infrared and Millimeter waves*, (K. Button, ed.) Vol 1. Academic Press, New York.

3) Petelin, M. I., 1974, On the theory of ultrarelativistic cyclotron self-resonance masers. *Izv Vuzov Radiofizika*, **17**, 902-908. (*Radiophys. Quantum Electron.*, **17**, 686-690).

4) Kanavets, V. I., and Klimov, O. I., 1976, The electron efficiency of a monotron and klystron with a relativistic polyhelical electron beam. *Radiotekhnika i Electronika*, **21**, 2359-2364. (*Radio Engng. Electron. Phys.*, **21**, 78-73).

5) Ginzburg, N. S., Zarnıtsyna, I. G., and Nusinovich, G. S., 1981, Theory of relativistic cyclotron-resonance maser amplifiers. *Izv. Vssh. Ucheb. Zaved., Radiofizika*, **24**, 481-490. (*Radiophys. Quant. Electron.*, **24**, 331-338).

6) Vomvoridis, J. L., 1982, An efficient Doppler-shifted electron-cyclotron maser oscillator. *Int J. Electron.*, **53**, 555-571.

7) Bratman, V. L., Ginzburg, N. S., Nusinovich, G. S., Petelin, M. I., and Strelkov, P. S., 1981, Relativistic gyrotrons and cyclotron autoresonance masers. *Int. J. Electron.*, **51**, 541-567.

8) Lin, A. T., 1984, Doppler shift dominated cyclotron masers. *Int. J. Electron.*, **57**, 1097-1107.

9) Lin, A. T., and Lin, C. C., 1985, Doppler shift dominated cyclotron maser amplifiers. *Int. J. Infrared Millimeter Waves*, **6**, 41-51.

10) Sprangle, P., Tang, C. M., and Serafim, P., 1985, Induced resonance electron cyclotron (IREC) masers. *Proc. 7th Int. FEL Conf.*, Tahoe City, California, U.S.A., 8-13 September.

11) Botvinnik, I. E., Bratman, V. L., Volkov, A. B., Denisov, G. G., Kol'chugin, B. D., and Ofitserov, M. M., 1982, Cyclotron-autoresonance maser with a wavelength of 2.4 mm. *Pis'ma Zh. Tekh. Fiz.*, **8**, 1386-1389. (*Sov. Tech. Phys. Lett.*, **8**, 596-597).

12) Botvinnik, I. E., Bratman, V. L., Volkov, A. B.,Ginzburg, N. S, Denisov, G. G., Kol'chugin, B. D., and Ofitserov, M. M., Petelin, M. I., 1982, *Pis'ma Zh. Eksp. Teor. Fiz.*, **35**, 418. (*JETP Lett.*, **35**, 516).

13) Bratman, V. L., Denisov, G. G., Ginzburg, N. S., and Petelin, M. I., 1983, FEL's with Bragg Reflection Resonators: Cyclotron Autoresonance Masers Versus Ubitrons. *I.E.E.E. J. Quant. Electron.*,**19** , 282.

14) Fliflet, A. W., 1986, Linear and non-linear theory of the Doppler-shifted cyclotron resonance maser based on TE and TM waveguide modes. *Int. J. Electronics*, VOL. **61**, NO 6, 1049-1080.

15) Gold, S. H., Fliflet, A. W., Manheimer, W. M., Black, W. M., Granatstein, V. L., Kinkead, A. K., Hardesty, D. L., and Sucy, M., 1985, High-voltage K_a-band gyrotron experiment. *IEEE Trans. on Plasma Science*, **PS-13**, No 6, 374-382.

16) McCowan, R. B., Fliflet, A. W., Gold, S. H., Granatstein, V. L., Wang, M. C., 1988, Design of a waveguide resonator with rippled-wall reflectors for a 100 GHz CARM oscillator experiment., *International Journal of Electronics*, To be published.

17) Herrmannsfeldt, W. B., 1979, SLAC Report *SLAC-226, UC-28 (A)*. Stanford University, Stanford, CA.

18) Finn, J. M., Fliflet, A. W., and Manheimer, W. M., 1986, One dimensional models for relativistic electron beam diode design. *Int. J. Electron.*, **61**, No 6, 985-1003.

19) Gold, S. H., Fliflet, A. W., Manheimer, W. M., McCowan, R. B., Black, W. M., Lee, R. C., Granatstein, V. L., Kinkead, A. K., Hardesty, D. L., and Sucy, M., 1987, High peak power K_a-band gyrotron oscillator experiment., *Phys. Fluids* ,**30**(7), p 2226-2238.

20) Adler, R. J., Kiuttu, G.F., Simpkins, B. E., Sullivan, D. J., and Voss, D. E., 1985, Improved electron emission by use of a cloth fiber cathode. *Rev. Sci. Instrumen.*, **56**, NO 5, 766-767.

21) Fink, J., Schilling, H. B., and Schumacher, U., 1980, Development and investigation of relativistic electron beams with finite energy spread and improved emittance. *J. Appl. Phys.*, **51**, NO 6, 2995-3000.

22) Kirkpatrick, D. A., Shefer, R. E., and Bekefi, G., 1985,High brightness electrostatically focused field emission gun for free electron laser applications. *J. Appl. Phys.*, **57**, NO 11, 5011-5016.

Table I: NRL 10υ GHZ carm oscillator parameters

Beam Voltage	600 kV
Beam Current	200 A
Pulse Length	50 nsec
Magnetic Field	25 kG
Phase Velocity	1.17c
Ω_c	32 GHz
$\alpha \equiv v_\perp / v_z$	0.6
Efficiency	20%
Power	24 MW
Operating Mode	TE_{61}
Cavity Parameters:	
Mean Wall Diameter	1.59 cm
Upstream Reflector	
Length	~3 cm (18 periods)
Ripple Depth	0.25 mm
Ripple Period	1.68 mm
Reflectivity	99%
Downstream Reflector	
Length	~1.5 cm (9 periods)
Ripple Depth	0.31 mm
Ripple Period	1.68 mm
Reflectivity	90%
Center Section Length	2.6 cm
Cavity Q	1500

CARM DISPERSION RELATION

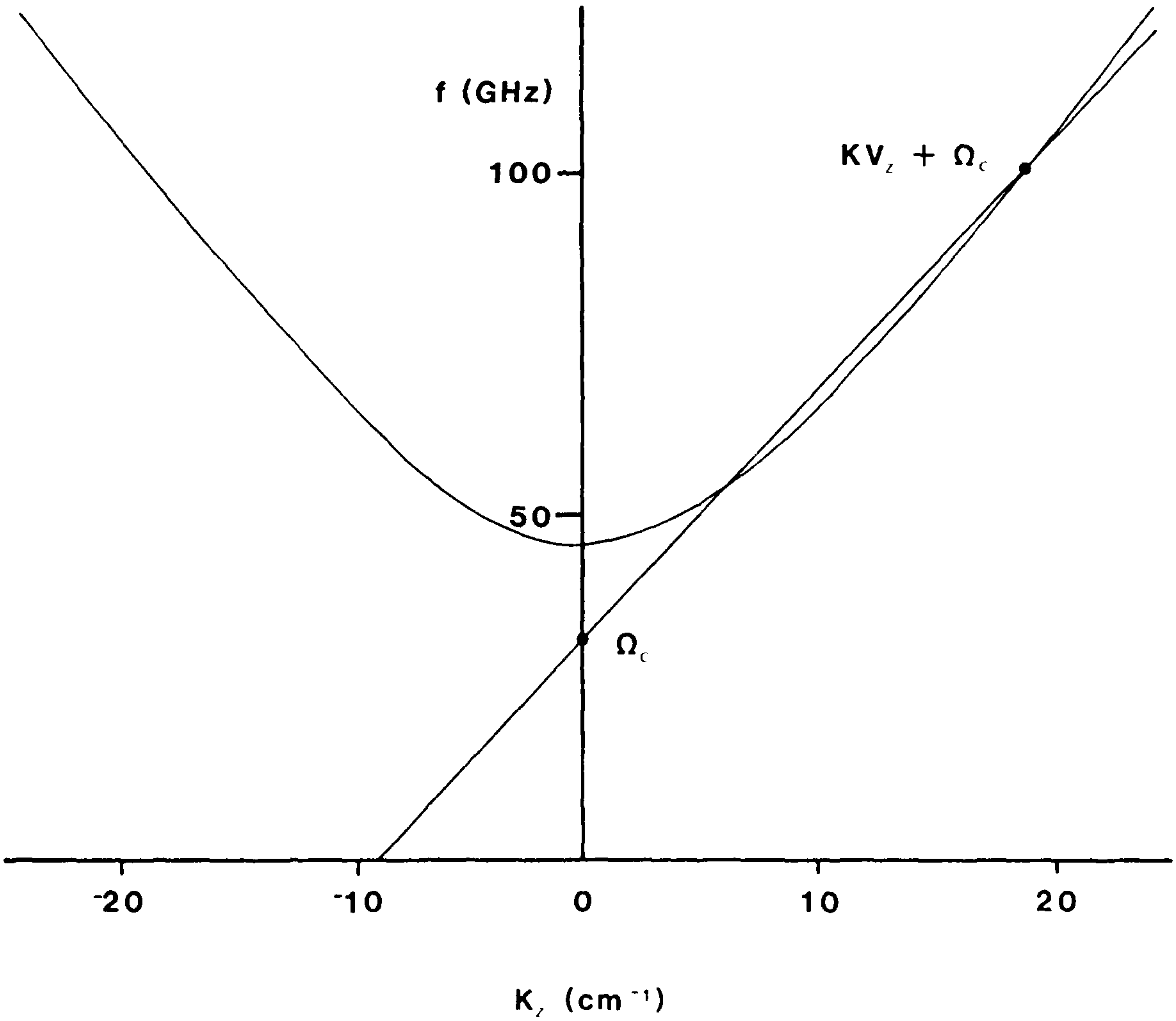

Fig. 1. The dispersion relation for the NRL 100 GHz. CARM experiment. The high frequency intersection of the electron beam line with the TE_{61} waveguide dispersion relation is the CARM operating regime. The lower frequency intersection is a competing gyrotron mode.

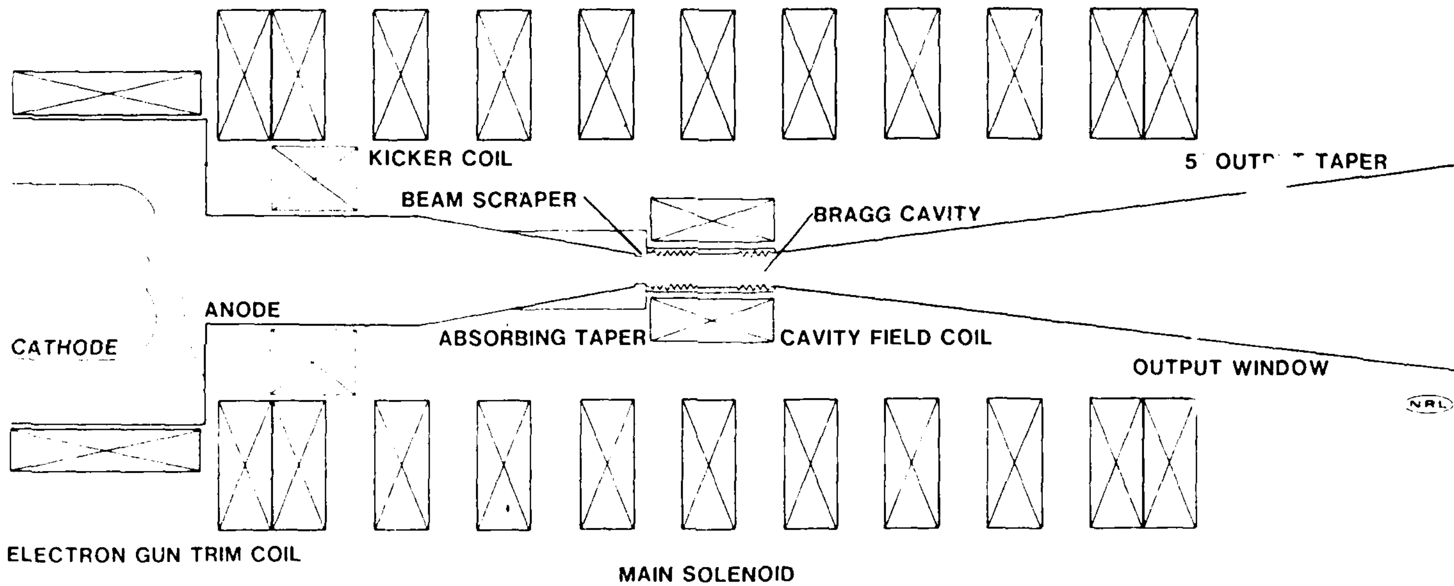

Fig. 2. Schematic of the CARM oscillator experiment

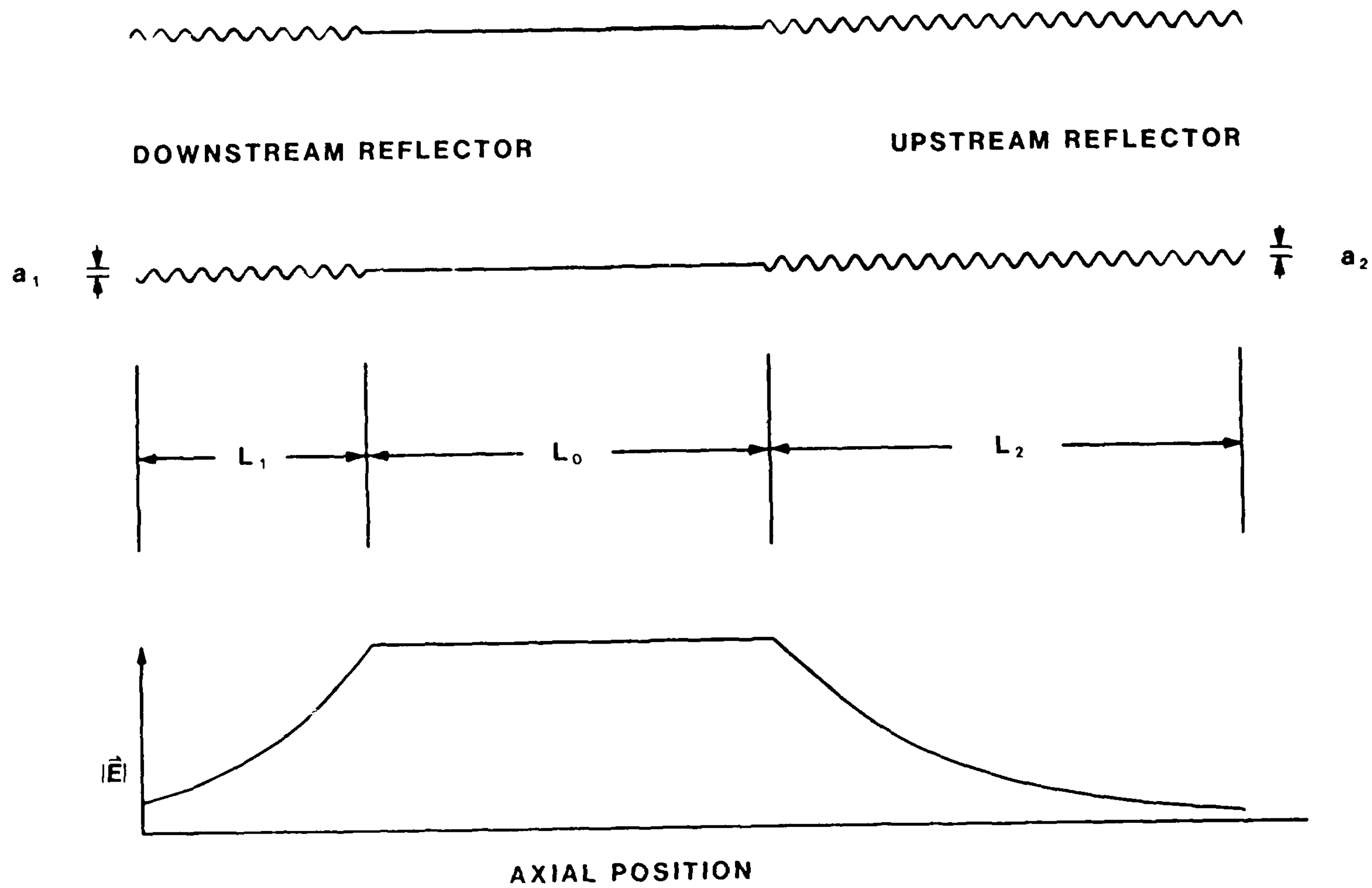

Fig. 3. The geometry of the CARM cavity with the electric field amplitude profile.

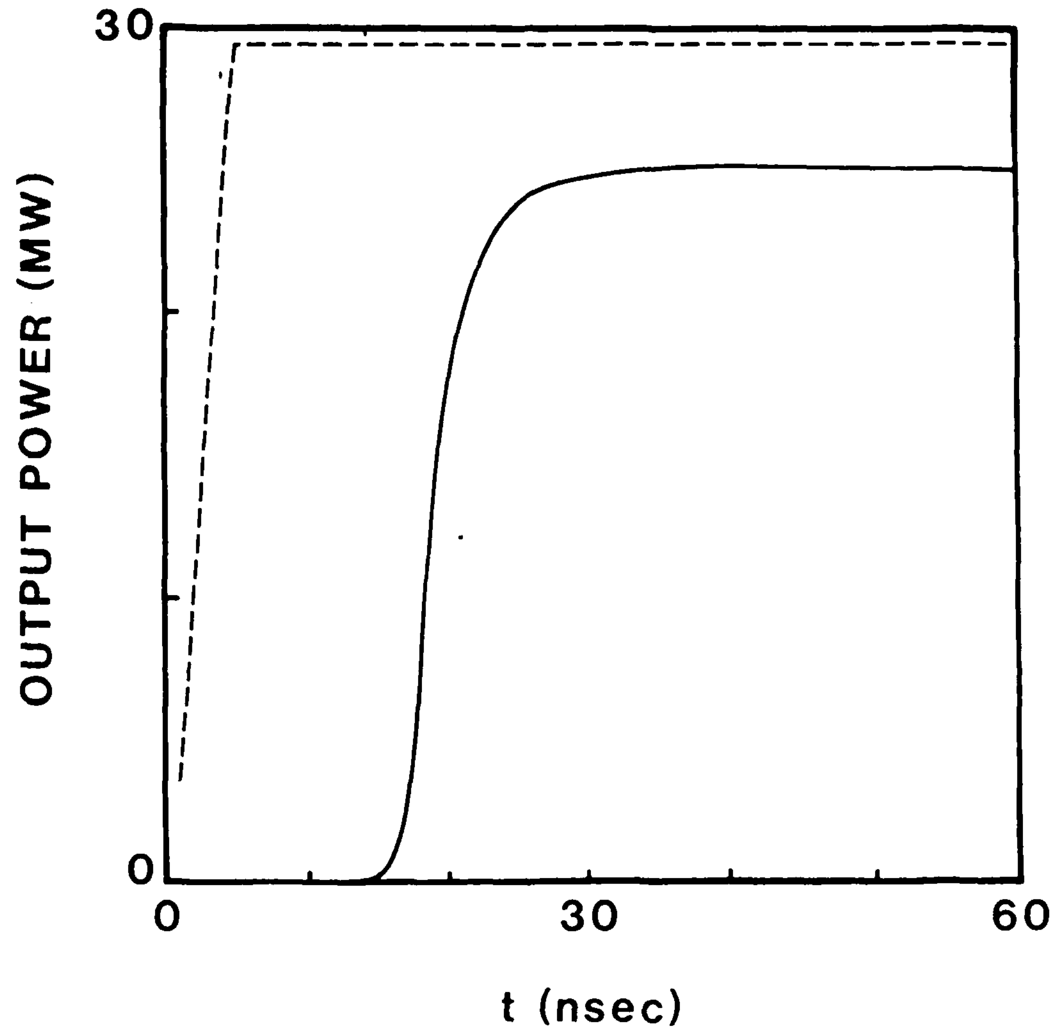

Fig. 4. Results of the time-dependent CARM oscillator code show that the 70 nsec pulse should be sufficient to drive the interaction to saturation. The dashed line represents the voltage waveform.

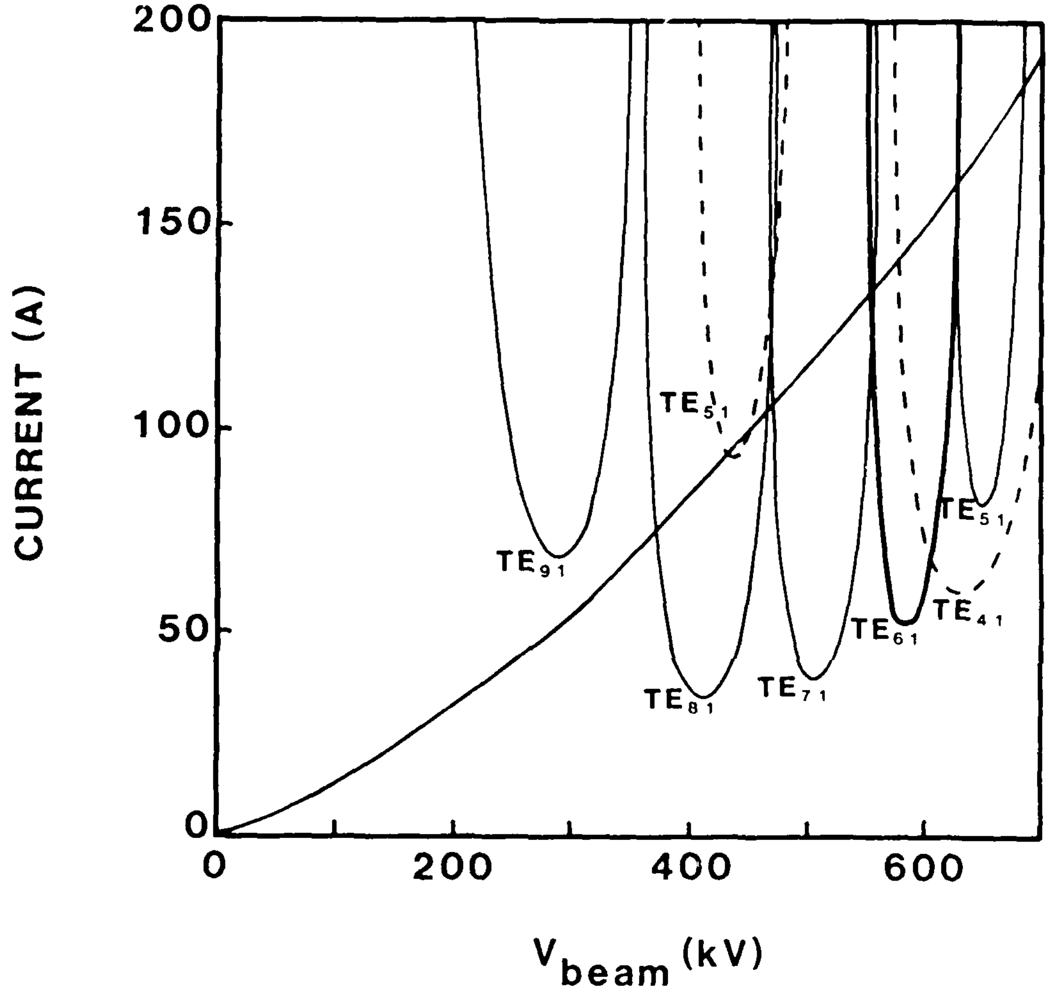

Fig. 5. Oscillation threshold currents for modes in the Bragg cavity for an electron beam with α=0.6 and a Langmuir-Child current-voltage behavior of the electron beam.

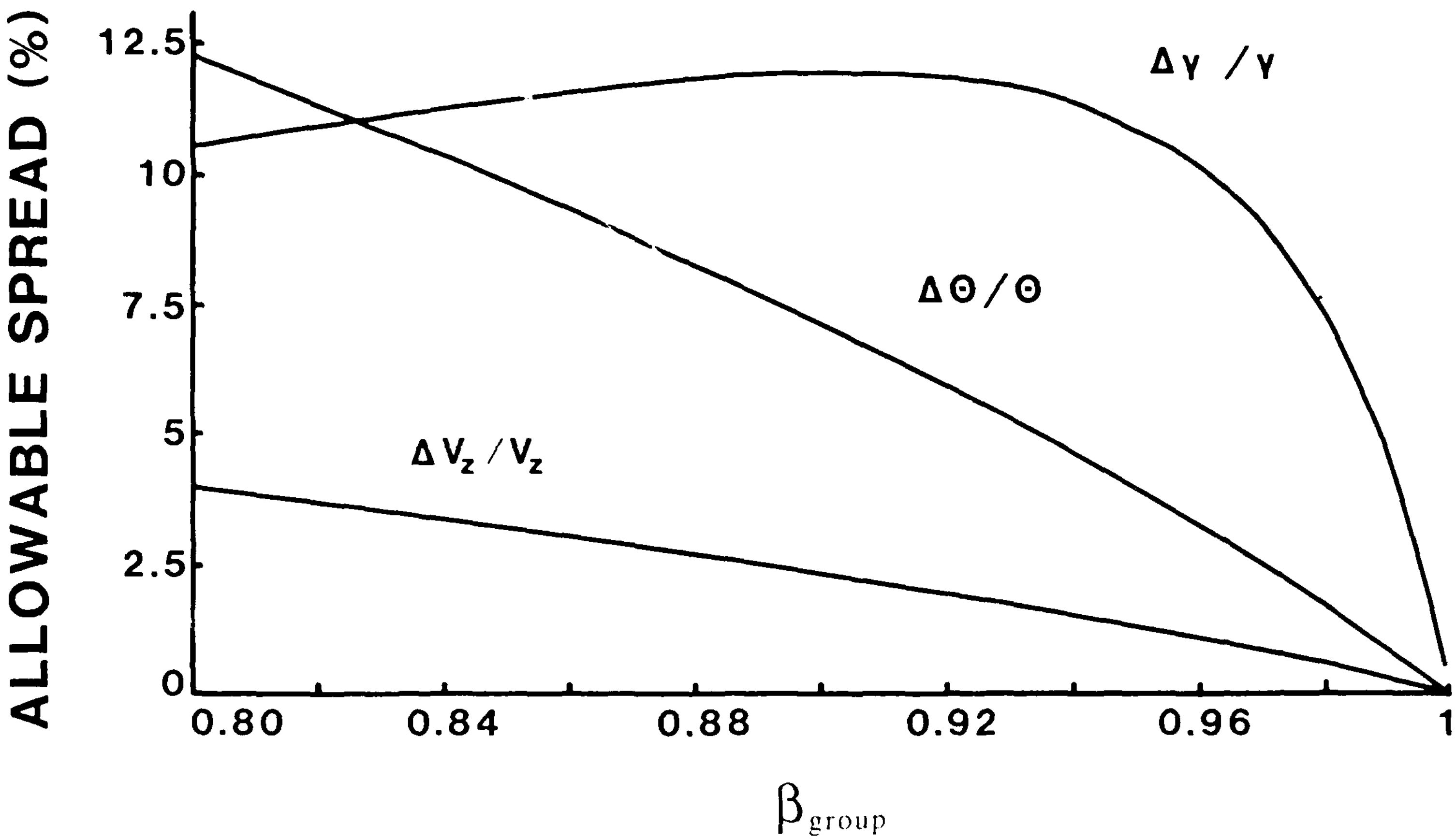

Fig. 6. The constraints on beam quality for high-efficiency CARM operation. If the beam quality is kept within these constraints the interaction will operate at nearly peak theoretical efficiency.

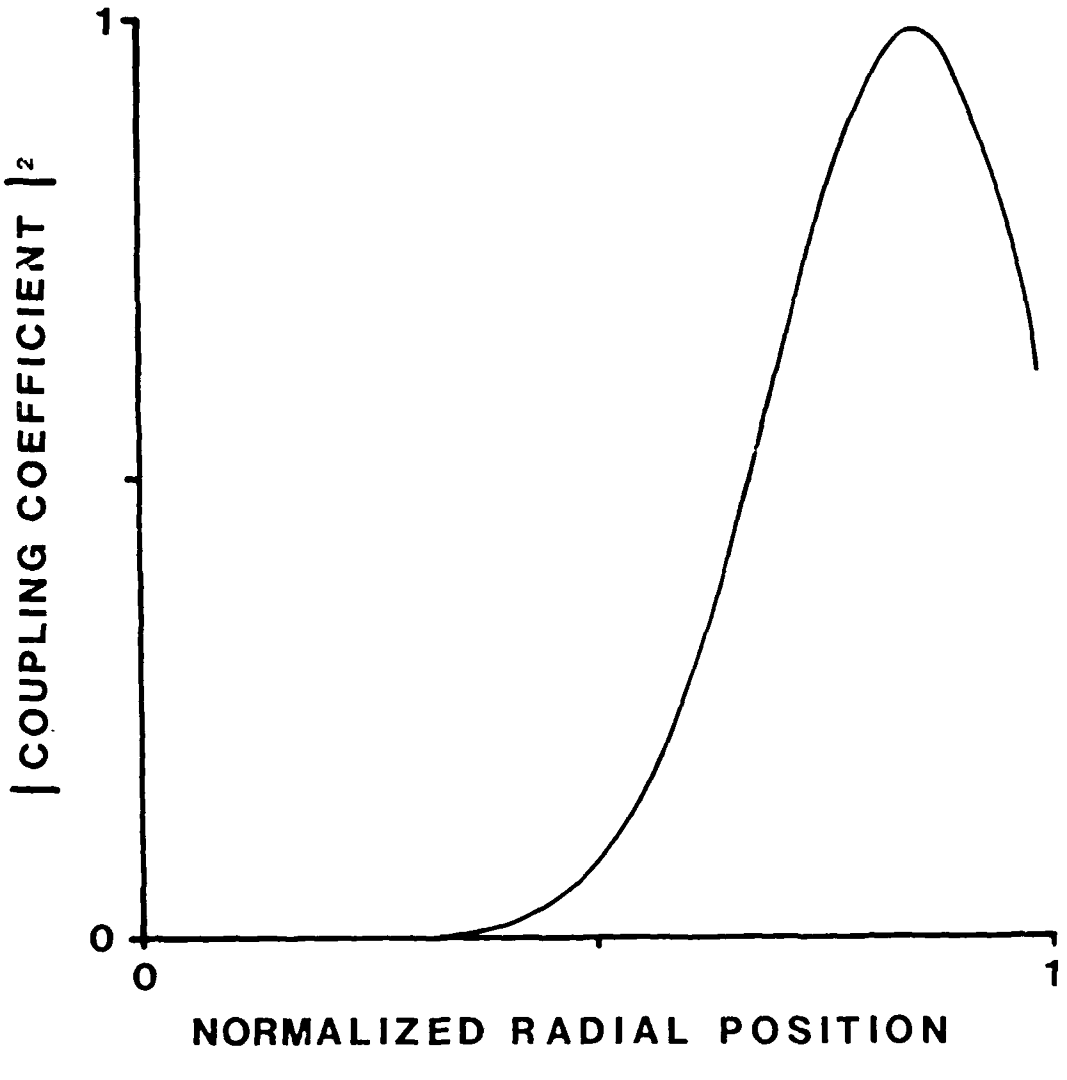

Fig. 7. The beam-wave coupling coefficient for the TE_{61} mode as a function of radial beam position.

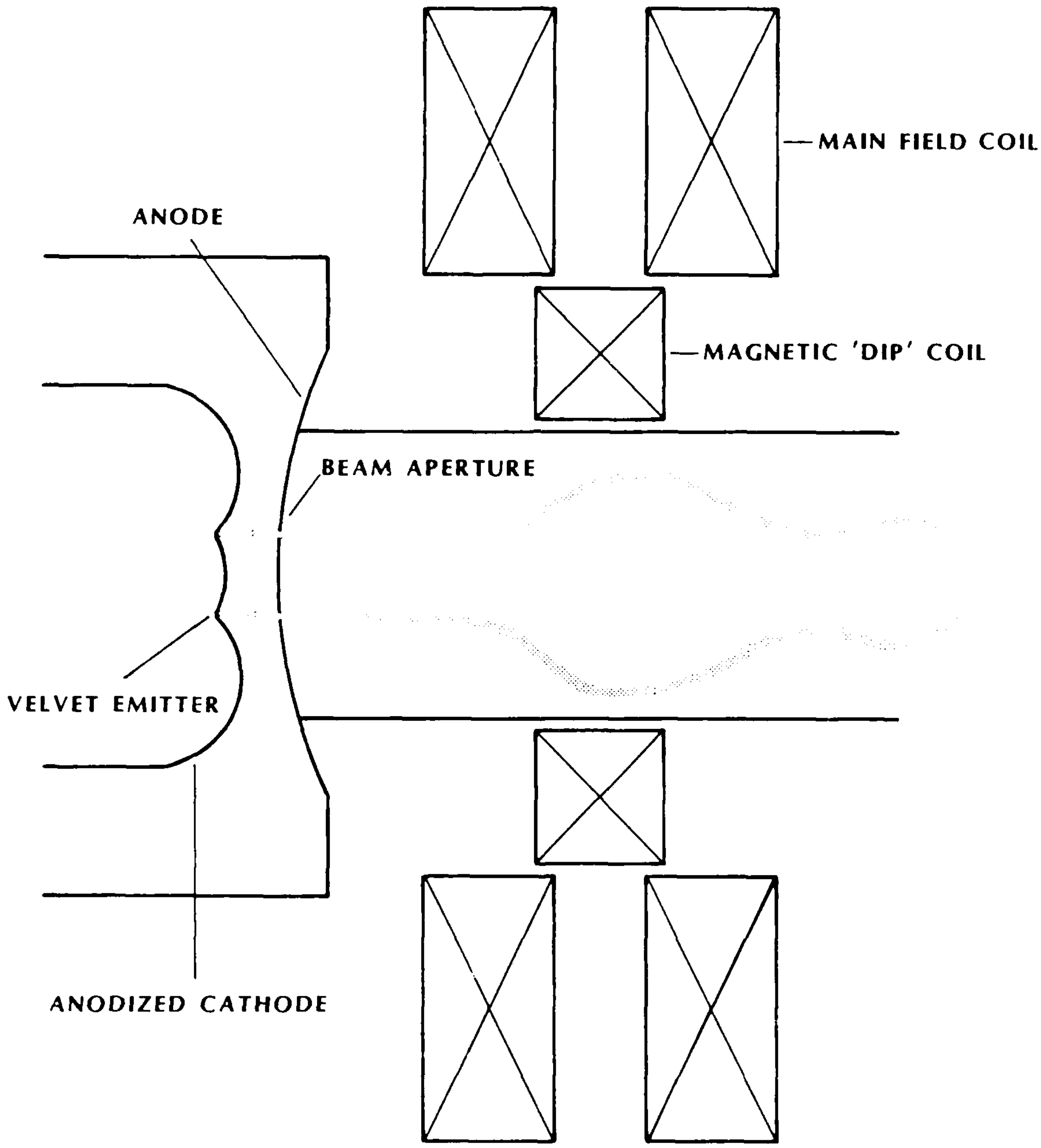

Fig. 8. Outline shape of the electron gun.

<u>4740 DISTRIBUTION LIST</u>

Air Force Avionics Laboratory AFWAL/AADM-1 Wright/Patterson AFB, Ohio 45433 Attn: Walter Friez	1 copy
Air Force Office of Scientific Research Bolling AFB Washington, D.C. 20332 Attn: H. Schlossberg	1 copy
Air Force Weapons Lab Kirkland AFB Albuquerque, New Mexico 87117 Attn: Dr. William Baker	2 copies
Columbia University 520 West 120th Street Department of Electrical Engineering New York, N.Y. 10027 Attn: Dr. S.P. Schlesinger	1 copy
A. Sen	1 copy
Columbia University 520 West 120th Street Department of Applied Physics and Nuclear Engineering New York, New York 10027 Attn: T.C. Marshall	1 copy
R. Gross	1 copy
Cornell University School of Applied and Engineering Physics Ithica, New York 14853 Attn: Prof. Hans H. Fleischmann	1 copy
John Nation	1 copy
R. N. Sudan	1 copy
Dartmouth College 18 Wilder, Box 6127 Hanover, New Hampshire 03755 Attn: Dr. John E. Walsh	1 copy
Department of Energy The Pentagon Washington, D.C. 20545 Attn: C. Finfgeld/ER-542, GTN	1 copy
T.V. George/ER-531, GTN	1 copy
D. Crandall/ER-55, GTN	1 copy

Defense Advanced Research Project Agency/DEO	
1400 Wilson Blvd.	
Arlington, Virginia 22209	
Attn: Dr. S. Shey	1 copy
Dr. L. Buchanan	1 copy
Defense Communications Agency	
Washington, D.C. 20305	
Attn: Dr. Pravin C. Jain	
Assistant for Communications	
Technology	1 copy
Defense Nuclear Agency	
Washington, D.C. 20305	
Attn: Mr. J. Farber	1 copy
Mr. Lloyd Stossell	1 copy
Dr. Leon Wittwer (RAAE)	5 copies
Defense Technical Information Center	
Cameron Station	
5010 Duke Street	
Alexandria, Virginia 22314	2 copies
Georgia Tech. EES-EOD	
Baker Building	
Atlanta, Georgia 30332	
Attn: Dr. James J. Gallagher	1 copy
Hanscomb Air Force Base	
Stop 21, Massachusetts 01731	
Attn: Lt. Rich Nielson/ESD/INK	1 copy
Hughes Aircraft Co.	
Electron Dynamics Division	
3100 West Lomita Boulevard	
Torrance, California 90509	
Attn: J. Christiansen	1 copy
J.J. Tancredi	1 copy
KMS Fusion, Inc.	
3941 Research Park Dr.	
P.O. Box 1567	
Ann Arbor, Michigan 48106	
Attn: S.B. Segall	1 copy
Lawrence Livermore National Laboratory	
P.O. Box 808	
Livermore, California 94550	
Attn: Dr. D. Prosnitz	1 copy
Dr. T.J. Orzechowski	1 copy
Dr. J. Chase	1 copy

Los Alamos Scientific Laboratory P.O. Box 1663, AT5-827 Los Alamos, New Mexico 87545	
Attn: Dr. J.C. Goldstein	1 copy
Dr. T.J.T. Kwan	1 copy
Dr. L. Thode	1 copy
Dr. C. Brau	1 copy
Dr. R. R. Bartsch	1 copy
Massachusetts Institute of Technology Department of Physics Cambridge, Massachusetts 02139	
Attn: Dr. G. Bekefi/36-213	1 copy
Dr. M. Porkolab/NW 36-213	1 copy
Dr. R. Davidson/NW 16-206	1 copy
Dr. A. Bers/NW 38-260	1 copy
Dr. K. Kreischer	1 copy
Massachusetts Institute of Technology 167 Albany St., N.W. 16-200 Cambridge, Massachusetts 02139	
Attn: Dr. R. Temkin/NW 14-4107	1 copy
Spectra Technologies- 2755 Northup Way Bellevue, Washington 98004	
Attn: Dr. J.M. Slater	1 copy
Mission Research Corporation Suite 201 5503 Cherokee Avenue Alexandria, Virginia 22312	
Attn: Dr. M. Bollen	1 copy
Dr. Tom Hargreaves	1 copy
Mission Research Corporation 1720 Randolph Road, S.E. Albuquerque, New Mexico 87106	
Attn: Dr. Ken Busby	1 copy
Mr. Brendan B. Godfrey	1 copy
SPAWAR Washington, D.C. 20363	
Attn: E. Warden Code PDE 106-3113	1 copy
G. Bates PMW 145	1 copy
Naval Research Laboratory Addressee: Attn: Name/Code	
Code 1001 - T. Coffey	1 copy
Code 1220 - Security	1 copy
Code 2628 - TID Distribution	22 copies
Code 4000 - W. Ellis	1 copy
Code 4700 - S. Ossakow	26 copies

Code 4700.1 - A.W. Ali	1 copy
Code 4710 - C. Kapetanakos	1 copy
Code 4740 - Branch Office	25 copies
Code 4740 - W. Black	1 copy
Code 4740 - A. Fliflet	1 copy
Code 4740 - S. Gold	1 copy
Code 4740 - A. Kinkead	1 copy
Code 4740 - W.M. Manheimer	1 copy
Code 4740 - M. Rhinewine	1 copy
Code 4770 - G. Cooperstein	1 copy
Code 4790 - B. Hui	1 copy
Code 4790 - C.M. Hui	1 copy
Code 4790 - Y.Y. Lau	1 copy
Code 4790 - P. Sprangle	1 copy
Code 5700 - L.A. Cosby	1 copy
Code 6840 - S.Y. Ahn	1 copy
Code 6840 - A. Ganguly	1 copy
Code 6840 - R.K. Parker	1 copy
Code 6840 - N.R. Vanderplaats	1 copy
Code 6850 - L.R. Whicker	1 copy
Code 6875 - R. Wagner	1 copy

Naval Sea Systems Command
Department of the Navy
Washington, D.C. 20362
Attn: Commander George Bates
PMS 405-300 — 1 copy

Northrop Corporation
Defense Systems Division
600 Hicks Rd.
Rolling Meadows, Illinois 60008
Attn: Dr. Gunter Dohler — 1 copy

Oak Ridge National Laboratory
P.O. Box Y
Mail Stop 3
Building 9201-2
Oak Ridge, Tennessee 37830
Attn: Dr. A. England — 1 copy

Office of Naval Research
800 N. Quincy Street
Arlington, Va. 22217
Attn: Dr. C. Roberson — 1 copy
Dr. W. Condell — 1 copy
Dr. T. Berlincourt — 1 copy

Office of Naval Research
1030 E. Green Street
Pasadena, CA 91106
Attn: Dr. R. Behringer — 1 copy

Optical Sciences Center University of Arizona Tucson, Arizona 85721 Attn: Dr. Willis E. Lamb, Jr.	1 copy
OSD/SDIO Washington, D.C. 20301-7100 Attn: IST (Dr. H. Brandt)	1 copy
Pacific Missile Test Center Code 0141-5 Point Muga, California 93042 Attn: Will E. Chandler	1 copy
Physical Dynamics, Inc. P.O. Box 10367 Oakland, California 94610 Attn: A. Thomson	1 copy
Physics International 2700 Merced Street San Leandro, California 94577 Attn: Dr. J. Benford	1 copy
Physical Science Inc. 603 King Street Alexandria, VA 22314 ATTN: M. Read	1 copy
Princeton Plasma Plasma Physics Laboratory James Forrestal Campus P.O. Box 451 Princeton, New Jersey 08544 Attn: Dr. H. Hsuan	2 copies
Dr. J. Doane	1 copy
Dr. D. Ignat	1 copy
Dr. H. Furth	1 copy
Dr. P. Efthimion	1 copy
Dr. F. Perkins	1 copy
Quantum Institute University of California Santa Barbara, California 93106 Attn: Dr. L. Elias	1 copy
Raytheon Company Microwave Power Tube Division Foundry Avenue Waltham, Massachusetts 02154 Attn: N. Dionne	1 copy

Sandia National Laboratories
ORG. 1231, P.O. Box 5800
Albuquerque, New Mexico 87185

Attn:	Dr. Thomas P. Wright	1 copy
	Mr. J.E. Powell	1 copy
	Dr. J. Hoffman	1 copy
	Dr. W.P. Ballard	1 copy
	Dr. C. Clark	1 copy

Science Applications, Inc.
1710 Goodridge Dr.
McLean, Virginia 22102

Attn:	Adam Drobot	1 copy
	P. Vitrello	1 copy
	D. Bacon	1 copy
	C. Menyuk	1 copy

Stanford University
High Energy Physics Laboratory
Stanford, California 94305

Attn:	Dr. T.I. Smith	1 copy

TRW, Inc.
Space-and Technology Group
Suite 2600
1000 Wilson Boulevard
Arlington, VA 22209

Attn:	Dr. Neil C. Schoen	1 copy

TRW, Inc.
Redondo Beach, California 90278

Attn:	Dr. H. Boehmer	1 copy
	Dr. T. Romisser	1 copy

University of California
Physics Department
Irvine, California 92717

Attn:	Dr. G. Benford	1 copy
	Dr. N. Rostoker	1 copy

University of California
Department of Physics
Los Angeles, CA 90024

Attn:	Dr. A.T. Lin	1 copy
	Dr. N. Luhmann	1 copy
	Dr. D. McDermott	1 copy

University of Maryland
Department of Electrical Engineering
College Park, Maryland 20742

Attn:	Dr. V. L. Granatstein	1 copy
	Dr. W. W. Destler	1 copy

University of Maryland Laboratory for Plasma and Fusion Energy Studies College Park, Maryland 20742	
Attn: Dr. Tom Antonsen	1 copy
Dr. John Finn	1 copy
Dr. Jhan Varyan Hellman	1 copy
Dr. Baruch Levush	1 copy
Dr. John McAdoo	1 copy
Dr. Edward Ott	1 copy
University of Tennessee Dept. of Electrical Engr. Knoxville, Tennessee 37916	
Attn: Dr. I. Alexeff	1 copy
University of New Mexico Department of Physics and Astronomy 800 Yale Blvd, N.E. Albuquerque, New Mexico 87131	
Attn: Dr. Gerald T. Moore	1 copy
University of Utah Deparment of Electrical Engineering 3053 Merrill Engineering Bldg. Salt Lake City, Utah 84112	
Attn: Dr. Larry Barnett	1 copy
Dr. J. Mark Baird	1 copy
U. S. Naval Academy Annapolis, Maryland 21402-5021	1 copy
U. S. Army Harry Diamond Labs 2800 Powder Mill Road Adelphi, Maryland 20783-1145	
Attn: Dr. Howard Brandt	1 copy
Dr. Edward Brown	1 copy
Dr. Stuart Graybill	1 copy
Varian Associates 611 Hansen Way Palo Alto, California 94303	
Attn: Dr. H. Jory	1 copy
Dr. David Stone	1 copy
Dr. Kevin Felch	1 copy
Dr. A. Salop	1 copy
Varian Eimac San Carlos Division 301 Industrial Way San Carlos, California 94070	
Attn: C. Marshall Loring	1 copy

Yale University
Applied Physics
Madison Lab
P.O. Box 2159
Yale Station
New Haven, Connecticut 06520
Attn: Dr. N. Ebrahim 1 copy
Dr. I. Bernstein 1 copy

Records 1 copy

Cindy Sims Code 2634 1 copy